scientific reports

Check for updates

OPEN

Serum metabolomics analysis reveals potential biomarkers of penicillins-induced fatal anaphylactic shock in rats

Qianwen Shi[1,2], Shuhui Wang[1,2], Gege Wang[1,2], Tao Wang[1,2], Kaili Du[1,3,4], Cairong Gao[1,2], Xiangjie Guo[1,2,5], Shanlin Fu[1,2,6] & Keming Yun[1,2]✉

Immunoglobulin E (IgE)-mediated immediate hypersensitivity reactions are the most concerning adverse events after penicillin antibiotics (PENs) administration because of their rapid progression and potential for fatal outcome. However, the diagnosis of allergic death is a forensic challenge because it mainly depends on nonspecific characteristic morphological changes, as well as exclusion and circumstantial evidence. In this study, an untargeted metabolomics approach based on liquid chromatography-mass spectrometry (LC-MS) was used to screen potential forensic biomarkers of fatal anaphylactic shock induced by four PENs (benzylpenicillin (BP), amoxicillin (AMX), oxacillin (OXA), and mezlocillin (MEZ)), and analyzed the metabolites, metabolic pathway and the mechanism which were closely related to the allergic reactions. The metabolomics results discovered that a total of 24 different metabolites in all four anaphylactic death (AD) groups, seven of which were common metabolites. A biomarker model consisting of six common metabolites (linoleic acid, prostaglandin D2, lysophosphatidylcholine (18:0), N-acetylhistamine, citric acid and indolelactic acid) AUC value of Receiver Operating Characteristic (ROC) curve was 0.978. Metabolism pathway analysis revealed that the pathogenesis of PENs-induced AD is closely related to linoleic acid metabolism. Our results revealed that the metabolomic profiling has potential in PENs-induced AD post-mortem diagnosis and metabolic mechanism investigations.

Keywords Penicillin antibiotics, Biomarker, Metabolomics, Drug-induced anaphylactic death

PENs constitute the most important group of antibiotics and remain the first-line therapy for many infectious diseases due to its high antibacterial activity and low medical burden[1–3]. However, PENs allergy is self-reported by about 10% of the patients and 0.01–0.05% of patients experience fatal anaphylactic reaction[4]. Meanwhile, PENs are also the most common cause of drug-induced fatal anaphylaxis[5–8]. An established concept is that PENs can serve as haptens to induce IgE through irreversibly forming drug-protein conjugates in vivo[2,9]. On re-exposure, the drug-protein conjugate cross-links its IgE which bound to the high-affinity receptor and induces the degranulation of mast cells and basophils, and release of inflammatory mediators that induce urticaria, vasodilatation, increased vascular permeability, edema and bronchoconstriction, leading to cardiovascular failure, bronchospasm and even death[2,10].

Drug-induced AD easily leading to a series of legal issues, such as medical disputes. The post-mortem diagnosis of fatal anaphylaxis is challenging, however, since death is usually the consequence of asphyxia or rapid shock, there may not be sufficient time for specific features to appear, and the diagnosis is still based on exclusion and circumstantial evidence. The forensic pathologists often lack relevant information and face non-specific anatomical-histopathologic data, which prevents obtaining convincing identification results[11]. So far, experimental researches on tissues and body fluids using various detection systems have emphasized the importance of the functions and pathophysiological roles of mast cells, eosinophils, IgE, tryptase, histamine, etc., in allergic reactions. However, their specific, individual or synergistic effects have certain limitations in

[1]School of Forensic Medicine, Shanxi Medical University, Taiyuan 030001, P. R. China. [2]Shanxi Key Laboratory of Forensic Medicine, Shanxi 030600, P. R. China. [3]School of Basic Medicine, Shanxi Medical University, Taiyuan 030001, P. R. China. [4]Department of Pathology, Shanxi Medical University, Taiyuan 030001, P. R. China. [5]Translational Medicine Research Center, Shanxi Medical University, Taiyuan 030001, P. R. China. [6]Centre for Forensic Science, University of Technology Sydney, Sydney 2007, Australia. ✉email: yunkeming5142@163.com

formulating a diagnosis of certainty and/or high likelihood of anaphylaxis[11–14]. Therefore, there is an urgent need to search for new biomarkers to reach the post-mortem diagnosis of AD.

Untargeted metabolomics is an unbiased global method that investigates low-molecular-weight metabolites to profile endogenous metabolic alterations resulting from pathological and physiological changes[15,16]. Untargeted metabolomics can serve as a promising tool to investigate metabolic responses to various diseases, identify potential biomarkers for diagnosis or prognosis purposes, and discover toxicity-related or drug-related metabolic pathways[17–21]. To date, there are some researches that have applied metabolomics approaches to study metabolic changes in anaphylaxis models. Hu et al.[22] reported the serum metabolic profiling analysis of anaphylactic guinea pigs and identified 9 potential biomarkers for diagnosis purposes. Gu et al.[23] explored the changes in endogenous metabolites in urine of the rat model of Shuang-huang-lian injection induced allergic reaction and determined 15 potential biomarkers that may provide the evidence of allergy. Gao et al.[24] sought to elucidate anaphylaxis reactions triggered by the injection of an herbal medicine, Qingkailing injection. The results indicated that the pathogenesis of Qingkailing injection induced anaphylaxis is closely related to arachidonic acid metabolism. Zhang et al.[25] investigated the metabolic alterations of the three causes of death and found that creatinine may represent some specific metabolic changes in anaphylactic shock.

The new insights of metabolomics in the monitoring of the metabolic status of anaphylaxis help in understanding its pathophysiological processes and give new approaches to diagnosis. The use of metabolomics also opens the possibility of identifying some novel markers of forensic interest. However, to the best of our knowledge, metabolomics approaches have not been applied in biomarkers discovery for PENs-induced AD, which are the most common cause of drug-induced fatal anaphylaxis.

In this study, we established model of rats AD induced by four PENs with different side chains (see Supplementary Tab. S1 online) which are most frequently associated with human anaphylaxis fatality[6,26–28]. The metabolic profile of PENs-induced AD in rat serum were analyzed with liquid chromatography quadrupole-time of fight mass spectrometry (UPLC-Q-TOF-MS) in order to identify potential forensic biomarkers and aid post-mortem diagnosis of AD in forensic.

Results

Anaphylactic symptoms, biochemical parameters and pathological changes. After intravenous injection, the bovine serum albumin (BSA) and PENs-induced AD groups expressed typical clinical symptoms of anaphylaxis, for example wheezing, convulsion, unsteady gait, cyanosis and death, whereas the control, carrier protein and drug groups had no active systemic anaphylaxis symptoms. The mortality rate of rats in the PENs-induced AD groups within 30 min was over 75%, and the rats died within 1–8 min after challenged, while rats in the BSA group did not die within 30 min (see Supplementary Tab. S2 online). Randomly select eight deceased rats from each PENs-induced AD group for IgE, immunohistochemical detection of tryptase in lung tissue, and serum metabolomics analysis.

The IgE is a key molecule in the IgE-mediated anaphylaxis. Increased IgE levels can be supportive in the diagnosis of anaphylactic shock[11]. Our results showed that the serum IgE of rats in the carrier protein ($p < 0.05$), BSA ($p < 0.01$), and four PENs-induced AD groups ($p < 0.001$) significantly increased compared with the control group (Fig. 1A).

Tryptase is considered mainly a practical marker of mast cell activation[29]. Immunohistochemical results revealed degranulated tryptase expression in the lung tissues of rats with BSA and four PENs-induced AD groups, while no significant tryptase expression in the lung tissues of rats with control, carrier protein, and four drug groups (Fig. 1B-L).

Consequently, the symptoms after challenged, the significantly increased levels of IgE in serum and the expression of trypsin-positive particles in lung tissues of PENs-induced AD group rats indicated that we successfully established the PENs-induced AD animal model.

Multivariate analysis. In the data matrix, the data were subject to multivariate analysis tools (Principal Components Analysis (PCA) and Orthogonal Projections to Latent Structures Discrimination Analysis (OPLS-DA)). As shown in Fig. 2A, quality control (QC) samples were clustered together in PCA score plots, indicating that the method had good repeatability and system stability. Due to no visible separation of each group in PCA, the OPLS-DA model was sequentially established to maximize the discrimination among the classes of observations and explore potential biomarker candidates in more detail. For the ten comparative groups of control/carrier protein, control/BSA, control/BP, control/AMX, control/OXA, control/MEZ, control/BP-AD, control/AMX-AD, control/OXA-AD and control/MEZ-AD, their OPLS-DA score plots and corresponding validation plots were constructed (Fig. 2B-U). All parameters for these models were summarized in Supplementary Tab. S3 online. In our results, all values for Hotelling's T2 were 95%, Q2 were < 0, R2X were > 0.4, and R2 were > 0.5, indicating that the model is reliable.

Potential biomarkers. Venn diagrams were used to obtain overviews of the unique ions that were significantly altered in each PENs-induced AD groups (Fig. 3A-D). For the BP-AD, AMX-AD, OXA-AD and MEZ-AD groups, 134, 177, 104 and 123 unique differential features meeting the threshold requirements were selected (black rectangle in Fig. 3A-D) and assigned to 19, 11, 12 and 14 metabolites, respectively. Among them, 7 metabolites were common between the four groups (black rectangle in Fig. 3E). The identified metabolites included amino acids and derivatives, fatty acids, lipid mediators, excretion metabolites, bile acids, organic acid and purine/pyrimidine metabolites. The details of the identified metabolites were shown in the Supplementary Tab. S4 online.

Glutathione was decreased only in the BP-AD group, eicosapentaenoic acid (EPA), 2'-deoxyuridine, uric acid, L-valine and L-tryptophan were increased only in the BP-AD group. Oleic acid was increased only in the OXA-AD group, L-glutamic acid and lysophosphatidylcholine (LysoPC) (15:0) were increased only in the MEZ-AD group. L-arginine and creatine were decreased in the BP-AD, AMX-AD and OXA-AD groups. Arachidonic

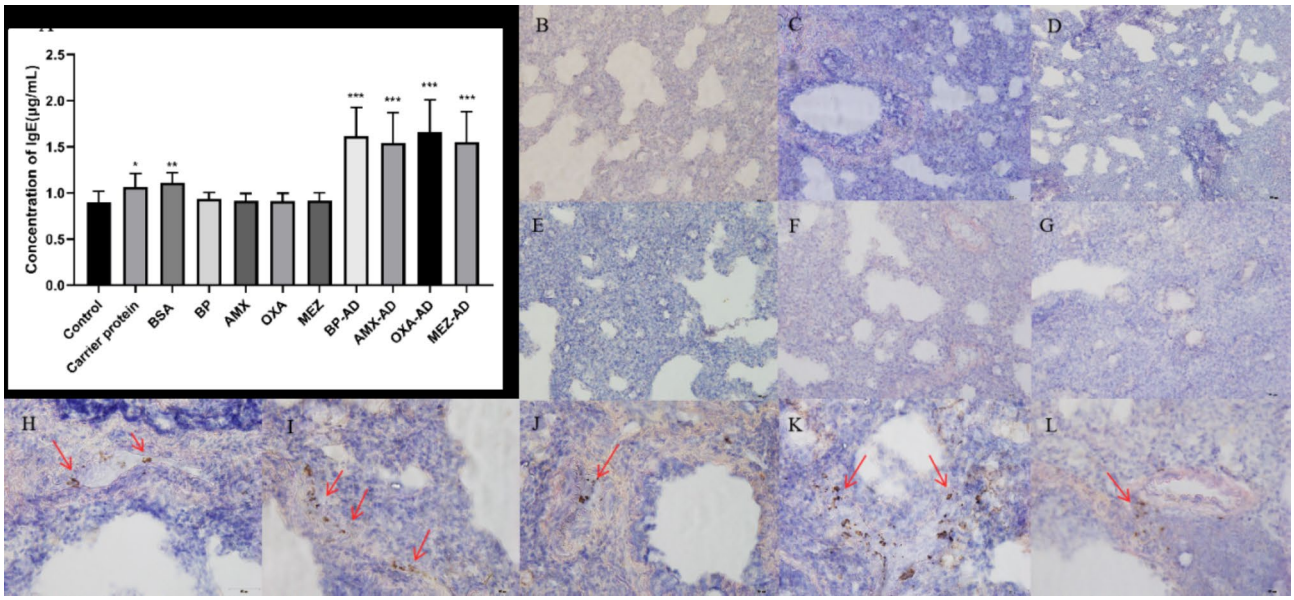

Fig. 1. Biochemical parameters and pathological changes in rats. (**A**) Levels of serum IgE in rats. (*$p < 0.05$, **$p < 0.01$, ***$p < 0.001$, versus the control group, respectively, $n = 8$). (**B-L**) Immunohistochemical findings of lung tissue in different groups ((**B**) control group; (**C**) carrier protein group; (**D**) BP group; (**E**) AMX group; (**F**) OXA group; (**G**) MEZ group; (**H**) BSA group; (**I**) BP-AD group; (**J**)AMX-AD group; (**K**) OXA-AD group; (**L**) MEZ-AD group; (**B-G**) ×200; (**H-L**) ×400). The positive reaction product of immunohistochemical staining was brown granules.

acid (AA) was increased in the BP-AD, AMX-AD and MEZ-AD groups. L-alanine was decreased in the BP-AD and OXA-AD groups. LysoPC (20:4(5Z,8Z,11Z,14)) and bilirubin were increased in the BP-AD and MEZ-AD groups. DL-pipecolic acid was increased in the OXA-AD and MEZ-AD groups. Sphingosine 1-phosphate (S1P) was increased in the AMX-AD and MEZ-AD groups. In the four PENs-induced AD groups, the levels of citric acid and uracil were decreased, while levels of linoleic acid (LA), prostaglandin D2 (PGD2), indolelactic acid (ILA), LysoPC (18:0) and N-acetylhistamine were increased. In order to express the clustering relationships between seven common differential metabolites and observe the trend, the peak areas of metabolites were used to construct heatmap (Fig. 3F).

For comparing the predictive ability of common metabolites, area under the curve (AUC), which combines the sensitivity (true positive rate) and specificity (false positive rate), was determined. ROC analysis showed that the common six metabolites in each PENs-induced AD groups had an AUC value more than 0.8 as well as having high sensitivity and specificity. The ROC curves for the evaluation of PENs-induced AD with the individual metabolites were shown in Fig. 4A-D. Because AD is a complex pathophysiological process that involves the systemic disorder of biochemical pathways, a biomarker panel containing a group of biomarkers could be more powerful to discriminate and provide relevant information. Therefore, a biomarker model consisting of the six metabolites was constructed. The results of 30% testing set showed that the accuracy of the model was 92.5% and AUC value of ROC curve was 0.978 (Fig. 4E). Confusion matrix of PENs-induced AD groups and control groups was shown in Fig. 4F, there is only one PENs-induced AD sample was incorrectly discriminated as the control group.

Pathway analysis. These biomarkers play an important role in specific metabolic pathways. Therefore, finding the disturbed metabolic pathways could help us to better understand the pathogenesis of PENs-induced AD. The pathways were picked based on pathway impact > 0.1 and $p < 0.05$. Perturbed metabolic pathways targeted by the four PENs-induced AD groups were shown in the Fig. 5A-D. It was found that several metabolic pathways (linoleic acid metabolism, arginine and proline metabolism, arachidonic acid metabolism) were significantly associated with PENs-induced AD and linoleic acid metabolism exhibited the most impact value (impact value = 1) with $p < 0.05$ (see Supplementary Tab. S5 online). Based on these results, the overall metabolic network maps of differential metabolites were constructed (Fig. 6).

Discussion

The present study focuses on PENs-induced AD, which represents the most frequent cause of drug-induced AD[5–7]. More remarkably, it is difficult to identification of anaphylactic death because it mainly depends on nonspecific characteristic morphological changes, as well as exclusion and circumstantial evidence. Therefore, the post-mortem diagnosis of anaphylactic death is a challenge for forensic pathologists. Biomarkers of anaphylactic death are urgently needed to develop more powerful diagnostic tools that identify bona fide anaphylactic death. The application of an untargeted metabolomics approach offers a great alternative because it is capable of detecting changes that occur within minutes (the time-frame of anaphylaxis) as opposed to proteomics and

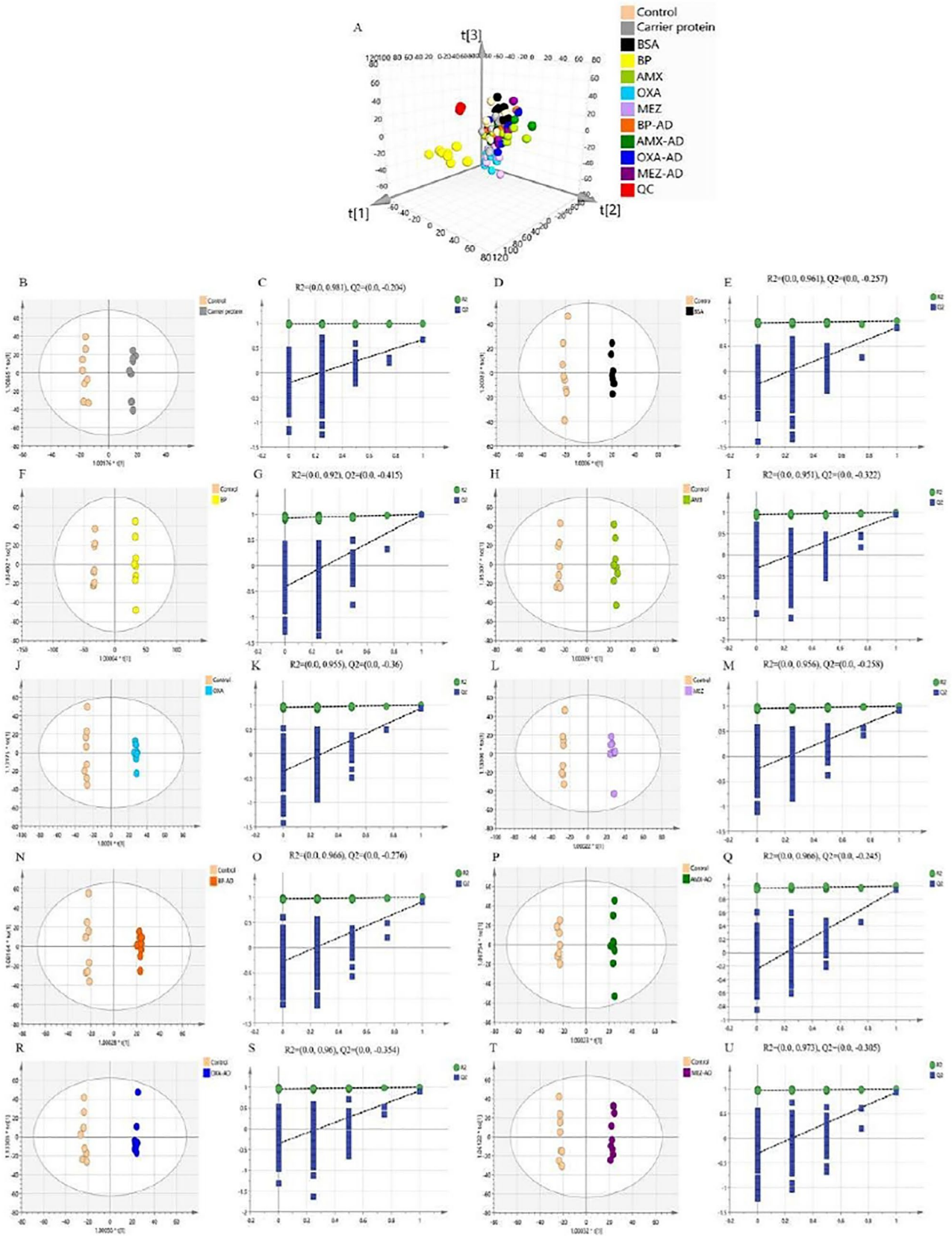

genomics markers, which generally take longer to express[30]. Previous studies have shown that the categories or concentrations of metabolites such as fatty acids, amino acids, pyrimidines, and glucose in the blood or urine had been changed during allergies[22–24]. Therefore, the metabolomics research could help to determine the post-mortem diagnosis of PENs-induced AD.

◂**Fig. 2**. Multivariate analysis. (**A**) The PCA score plot of control group (tan), carrier protein group (gray), BSA group (black), BP group (yellow), AMX group (lime), OXA group (sky blue), MEZ group (lavender), BP-AD group (orange), AMX-AD group (green), OXA-AD group (blue) and MEZ-AD group (violet) revealed a close clustering of quality control (QC) samples (red). (**B**) OPLS-DA for control/carrier protein comparative group. (**C**) Validation plots of OPLS-DA for control/carrier protein comparative group. (**D**) OPLS-DA for control/BSA comparative group. (**E**) Validation plots of OPLS-DA for control/BSA comparative group. (**F**) OPLS-DA for control/BP comparative group. (**G**) Validation plots of OPLS-DA for control/BP comparative group. (**H**) OPLS-DA for control/AMX comparative group. (**I**) Validation plots of OPLS-DA for control/AMX comparative group. (**J**) OPLS-DA for control/OXA comparative group. (**K**) Validation plots of OPLS-DA for control/OXA comparative group. (**L**) OPLS-DA for control/MEZ comparative group. (**M**) Validation plots of OPLS-DA for control/MEZ comparative group. (**N**) OPLS-DA for control/BP-AD comparative group. (**O**) Validation plots of OPLS-DA for control/BP-AD comparative group. (**P**) OPLS-DA for control/AMX-AD comparative group. (**Q**) Validation plots of OPLS-DA for control/AMX-AD comparative group. (**R**). OPLS-DA for control/OXA-AD comparative group. (**S**) Validation plots of OPLS-DA for control/OXA-AD comparative group. (**T**) OPLS-DA for control/MEZ-AD comparative group. (**U**) Validation plots of OPLS-DA for control/MEZ-AD comparative group.

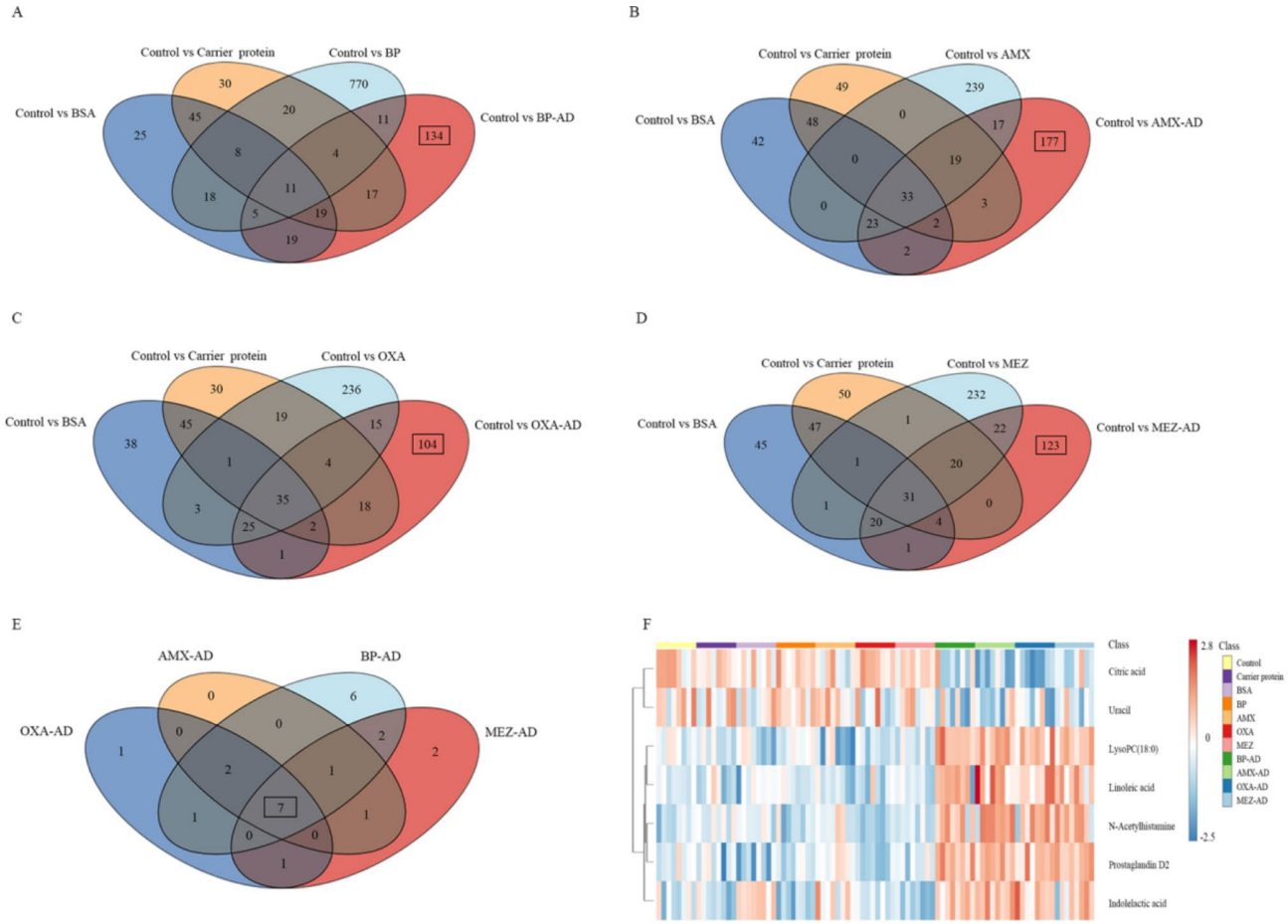

Fig. 3. Venn diagram and heatmap plot. (**A**) Venn diagram of unique differential features in the BP-AD group; (**B**) Venn diagram of unique differential features in the AMX-AD group; (**C**) Venn diagram of unique differential features in the OXA-AD group; (**D**) Venn diagram of unique differential features in the MEZ-AD group; (**E**) Venn diagram of common differential features in four PENs-induced AD groups; (**F**) Heatmap plot of the 7 common potential metabolites. Red color indicates a higher level and blue color indicates a lower level.

Firstly, we successfully established PENs (BP, AMX, OXA and MEZ) induced AD animal models in rats, which expressed typical clinical symptoms of anaphylaxis, high IgE level in serum and trypsin-positive particles in lung tissues after challenge with allergen on the 20th day of sensitization. Under our experimental conditions, the mortality of allergic reaction caused by PENs was greater than 75%, lower than the Park's experimental model, which may be related to the strain of rodent[31]. Subsequently, the metabolomics protocol was applied to investigate the effects of PENs-induced AD on the metabolites and relative metabolic pathways, and significant

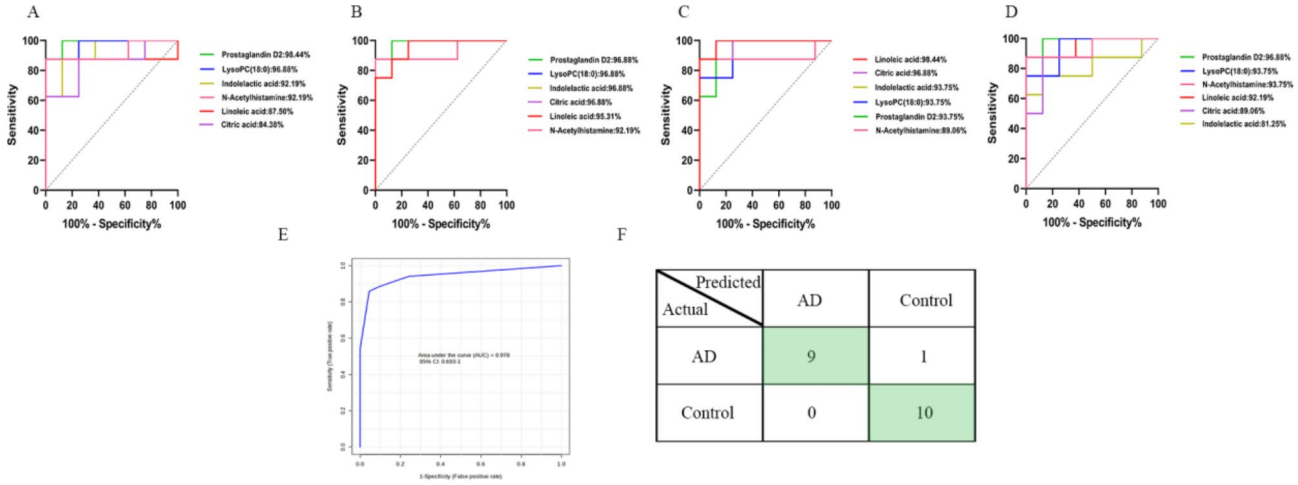

Fig. 4. ROC curves for evaluating PENs-induced AD with the individual metabolites (**A-D**) and the combination of the six metabolites (**E**) predicting model. (**F**) Confusion matrix of PENs-induced AD groups and control groups. (**A**) BP-AD group; (**B**) AMX-AD group; (**C**) OXA-AD group; (**D**) AMX-AD group.

differences were detected in metabolic profile between PENs-induced AD and control groups. The results showed that in the four PENs-induced AD groups, we obtained a total of 24 specific potential biomarkers excluding the effect of only-drugs, only-BSA and only-carrier proteins, six of which were common biomarkers and closely related to PENs-induced AD.

Metabolic changes in lipid metabolism in PENs-induced AD serum include an increase in LA, EPA, AA, LysoPCs, oleic acid and S1P, in particular, increases in LA and LysoPC(18:0) were found in all four PENs-induced AD groups. LA is an ω-6 polyunsaturated fatty acids (PUFAs)[32]. When cells are stimulated, LA is released from membrane phospholipids to form various derivatives involved in cell signaling[33]. Under desaturase, elongation and partial peroxisomal, LA can be transformed into AA and EPA. AA is a precursor of many inflammatory mediators. Some AA metabolites, such as prostaglandins are associated with the development of inflammation. We found that the AA metabolites were significantly altered in rats of PENs-induced AD groups compared with control group, especially an increase in PGD2. PGD2 is the major prostaglandins produced by activated mast cells. Accumulating evidence suggests a central role of the PGD2 in allergy development and progression[34–36]. PGD2 plays pro-inflammatory roles and induces chemotaxis in Th2 cells, neutrophils, eosinophils and basophils with enhanced degranulation[37–40]. Local application of PGD2 induces peripheral vasodilation, while systemic injection of PGD2 induces flushing and nasal congestion[38]. However, it has been suggested that PGD2 exerts a biphasic effect in anaphylaxis, a study in mice revealed that PGD2 attenuates vascular hyperpermeability by activation of the d-type prostanoid receptor 1 on endothelial cells and strengthening of endothelial barrier function playing a protective role in anaphylactic shock[41,42]. The effect of PGD2 in anaphylaxis is still inconclusive and needs further investigation. EPA is a kind of ω-3 PUFAs, and reported to competitively inhibit the formation of prostaglandins from AAs, and reduce the generation of cytokines and IgE related to allergy[43]. In the present study, LA and PGD2 were common differential metabolites in four PENs-induced AD group, suggesting that they were potential markers of AD induced by PENs.

LysoPC is a kind of lipid compound hydrolyzed from phosphatidylcholine. It has been shown that LysoPCs are associated with inflammation[44]. LysoPCs could activate the transcription factor NF-κB by stimulating toll-like receptors and G protein-coupled receptors and mediating the production of reactive oxygen species to induce inflammatory reactions[45,46].Besides, LysoPCs could also activate RhoA/ROCK signaling pathway to regulate vascular endothelial permeability, aggravate endothelial dysfunction and inflammation[47–49]. Moreover, LysoPCs are a source for the synthesis of AA and derivatives[50]. LysoPCs can also be indirectly converted into lipid mediator S1P, which has been described as an essential player in the immune response[51]. It is involved in the activation and degranulation of mast cells, and is related to bronchoconstriction and mucous secretion[52–54]. Our results demonstrated 3 LysoPCs, AA and S1P altered in AD, among them, LysoPC (18:0) was increased in all four PENs-induced AD groups. Jiang et al.found LysoPC (18:0) was positively correlated with the levels of cytokines such as IL-2, IL-4, IL-6 and IFN-γ, which is closely related to the mechanism of anaphylaxis[47]. Barber et al.also found that LysoPC (18:0) was increased in the severe allergic group[55]. Thus, the results suggest that LysoPC (18:0) is a potential biomarker associated with PENs-induced AD.

Histamine is one of the most important mediators secreted by mast cells and basophils, which can cause vasodilatation, bronchial spasm or myocardial depression, and is known as the "gold standard" for acute allergy monitoring. However, histamine has a very short half-life in serum and is rarely detectable, and sample degradation following death further interferes with postmortem analysis[56]. Our results showed that the histamine metabolites N-acetylhistamine were upregulated in four PENs-induced AD groups. Research has shown that injecting mice with more than 60 μg N-acetylhistamine can cause low temperature[57] and elevated N-acetylhistamine levels may be associated with trembling phenomenon in allergic BN rats[58]. This also showed that N-acetylhistamine could replace histamine as potential biomarkers for PENs-induced AD.

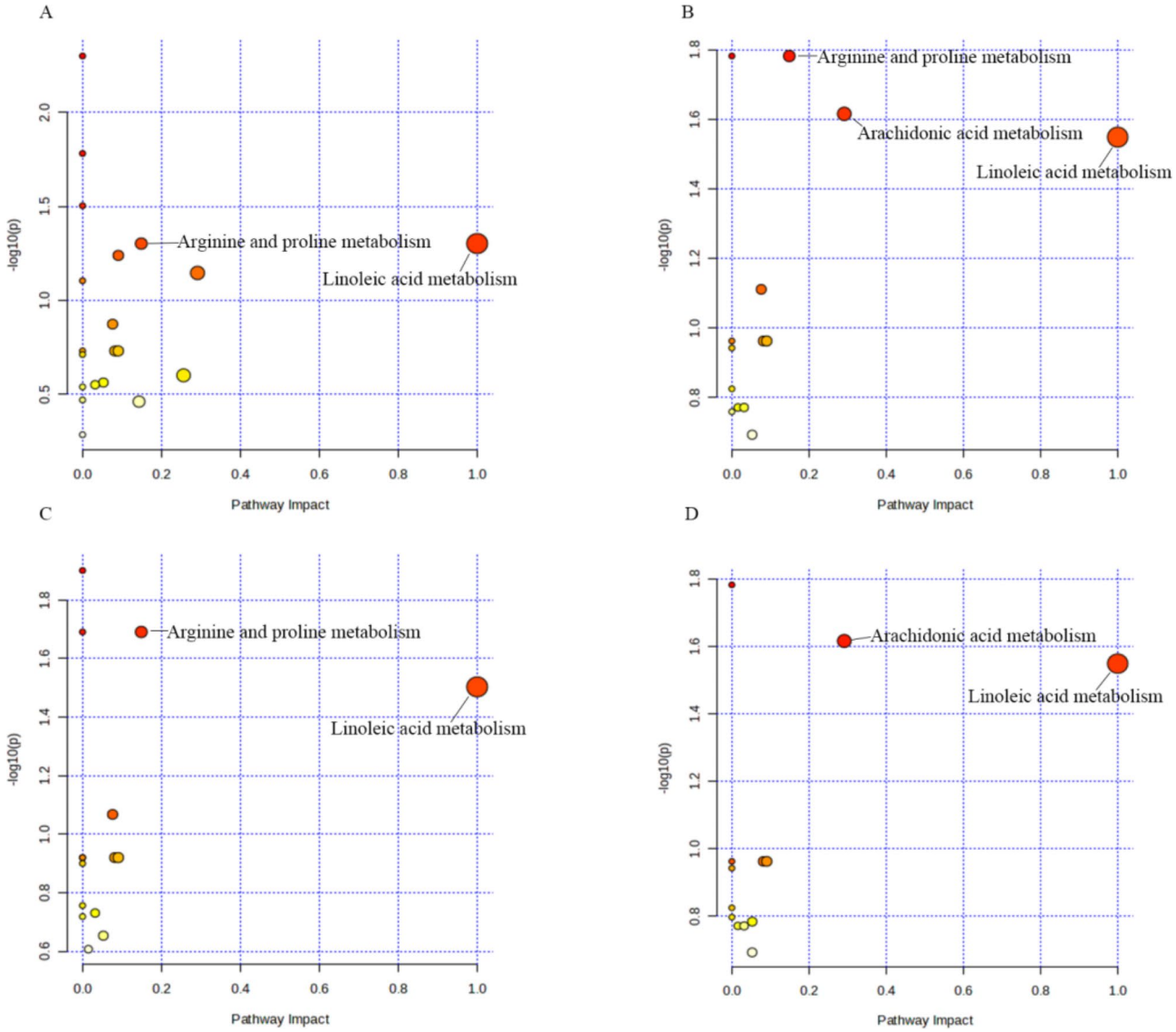

Fig. 5. The metabolic pathways of differential metabolites identified in four PENs-induced AD groups. Each dot of the figure represents a related metabolic pathway. The color and size of each dot was related to the-log (*p*) value and pathway impact value, respectively. (**A**) BP-AD group; (**B**). AMX-AD group; (**C**) OXA-AD group; (**D**) MEZ-AD group.

Citric acid serves as the primary substrate in the initiation of the tricarboxylic acid cycle (TCA). Anaphylaxis is an acute multisystem syndrome, it may lead to sudden energy expenditure. Such stress often promotes the TCA cycle to produce more ATP[22]. The lower levels of citric acid in the PENs-induced AD groups might be a result of high energy expenditure in the anaphylaxis reaction. Moreover, as an acidic substance, citric acid may play a role in maintaining acid-base balance within organism.

ILA is a bacterial tryptophan metabolism produces effective bioactive metabolite. It has been reported that ILA inhibited the lipopolysaccharides-induced upregulation of allergy-related cytokines in macrophages and reduced the mRNA expression of allergy-related interleukins. ILA was also positively correlated with complement factor H-related protein 4 in the plasma, which could activate mast cells to promote allergies by activating the complement pathway[59,60].It suggested that the gut microbiota plays an important role in anaphylaxis and the increase of ILA might be involved in the pathogenesis of allergy.

In summary, the present study revealed abnormal metabolites of AD induced by PENs, providing information for the exploration of anaphylaxis pathogenesis. These results demonstrated that a combination of 6 common metabolites (LA, PGD2, LysoPC (18:0), N-acetylhistamine, citric acid and ILA) might be the potential biomarker for post-mortem identification of PENs-induced AD. However, this study has some limitations. The models were constructed based on animal data. Thus, large scale autopsy samples are needed to verify the applicability of the diagnosis PENs-induced AD in future research. Furthermore, due to the capabilities of LC-MS detectors and

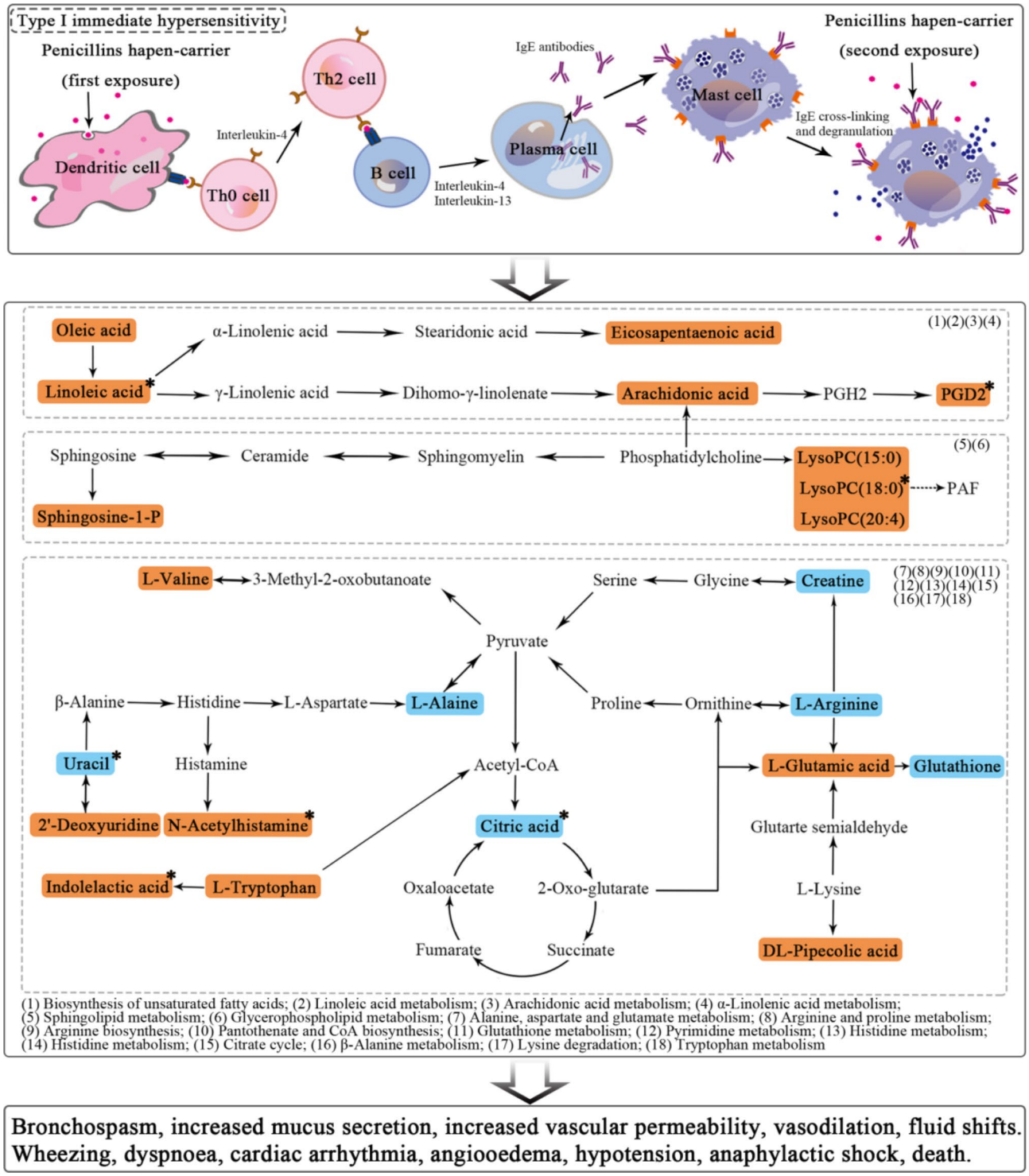

Fig. 6. The perturbed metabolic pathways associated with PENs-induced AD.
Orange and blue indicate an increase and decrease in the levels of metabolite, respectively. *: The common metabolites in the four PENs-induced AD groups. The mechanism of type I immediate hypersensitivity to PENs adapted from Castells[2].

records of databases, the metabolites we focused upon and could identify were very limited. Further research into these specific metabolites needs to be undertaken to establish exact concentrations reached.

Conclusion

In conclusion, our study identified a combination of 6 metabolites indicators with potential predictive value for PENs-induced AD and explored their major potential metabolic pathway based on the KEGG pathway maps.

We were the first to study the mechanism of PENs-induced AD at the metabolic level. The results of this study revealed that LC-MS-based metabolic profiling analysis might be an effective tool for investigating metabolic alterations in the procedure of death and diagnosing of the cause of death on account of metabolic features. It is helpful to determine the cause of death in complicated cases for forensic practice.

Materials and methods

Statement of ethics and regulations. We report the current study in accordance with ARRIVE guidelines (https://arriveguidelines.org). All animal experiments were performed in accordance with the applicable Chinese legislation and approved by the Institute of Zoology Animal and Medical Ethics Committee, Shanxi Medical University (No: 2021aLL051). All methods were performed in accordance with the relevant guidelines and regulations.

Chemical and reagents. BP, AMX, OXA, and MEZ were obtained from Huabei Pharmaceutical (Hebei, CHN), BSA, ovalbumin (OVA) were supplied by Sigma-Aldrich (St. Louis, MO, USA). Aluminum hydroxide gel (AHG) was purchased from Solarbio (Beijing, CHN). 2-chloro-L-phenylalanine was obtained from Aladdin Chemistry (Shanghai, China). Deionized water was obtained from a Milli-Q purification system (Millipore, Bedford, MA, USA). Acetonitrile (MeCN) and methanol (MeOH) were purchased from Sigma Aldrich (Saint Quentin Fallavier, France). Formic acid (HCOOH) 98% was purchased from Tianjin Damao Chemical Reagent Factory (Tianjin, China). All solvents were analytical grade. IgE enzyme-linked immunosorbent assay (ELISA) kit was purchased by Jiangsu Meimian Industrial Co., Ltd (Yancheng, CHN). KeyGen one-step immunohistochemistry (IHC) assay kit was purchased by KeyGen Biotech (Nanjing, CHN), rabbit anti-mast cell tryptase was purchased by BIOSS (Beijing, CHN).

Synthesis of BSA and OVA drug-hapten conjugates. Drug-hapten conjugates were prepared in order to sensitize rats for allergen challenges. Four different haptens, BP, AMX, OXA, and MEZ, were used with two different protein carriers, BSA and OVA. BSA conjugates were injected into rats to sensitize animals while OVA conjugates were used to perform allergen challenges. Conjugates (BP-BSA, BP-OVA, AMX-BSA, AMX-OVA, OXA-BSA, OXA-OVA, MEZ-BSA, and MEZ-OVA) were prepared by the method of Park[31]. Briefly, four drugs were conjugated to OVA and BSA by dissolving 50 mg of BSA or OVA in 11 mL of 8 mM veronal buffer (pH 8.5) and then adding 2000 mg of BP, AMX, OXA, or MEZ that was dissolved in veronal buffer. The pH was maintained between 8.5 and 9.0 by addition of 1 N NaOH. These compounds reacted under mild stirring over 24 h at 37 ℃. The reaction mixture was centrifuged, and the supernatant was filtered using a 10 kDa membrane filtration to remove excess drugs. Aliquots of the dialyzed supematant (10 mg/mL) were stored at -20 ℃. In order to determine conjugation efficiency, we used a penmaldate assay from Levine et al.[61] The BP-BSA, BP-OVA, AMX-BSA, AMX-OVA, OXA-BSA, OXA-OVA, MEZ-BSA, and MEZ-OVA contained 11, 15, 14, 12, 9, 7, 9 and 20 hapten groups per mole of protein, respectively.

Animals and administration. Healthy adult Sprague-Dawley rats ($n=120$; all males, 180–200 g; Permission for Laboratory Animal Use: SCXK-2019-0010) were purchased from the Beijing Changyang Xishan Farm (Beijing, China). The rats were kept in the room at 24 ± 2 ℃ and 55 ± 5% humidity with a 12 h/12 h light/dark cycle. The rats were allowed free access to food and water and were acclimated to the room for 1 week. The euthanasia method was excessive anesthesia according to the AVMA Guidelines for the Euthanasia of Animals (2020 Edition).

An animal model is established based on previous research method[22,31,62] with some modifications. Generally, the success rate of animal allergic reaction models is not 100% due to the individual differences in rats. Therefore the rats were randomly divided into eleven groups: a control group, a carrier protein group, a BSA group, a BP group, a AMX group, a OXA group, and a MEZ group ($n=8$); a BP-AD group, a AMX-AD group, a OXA-AD group, and a MEZ-AD group ($n=16$). The rats in the control, BP, AMX, OXA, MEZ groups were intraperitoneal injection (ip) of 1mL of normal saline (NS), BP (90 kU/kg), AMX (90 mg/kg), OXA (357.1 mg/kg) or MEZ (178.6 mg/kg) on days 1, 3 and 5 and intravenous injection (iv) of NS, BP, AMX, OXA or MEZ at the same doses on day 20, respectively. The drug dose of the rats in BP, AMX, OXA and MEZ groups were derived using pharmacological conversion factor[63] from adult human clinical maximum dose. The rats in the carrier protein, BSA, BP-AD, AMX-AD, OXA-AD, and MEZ-AD groups were immunized by intraperitoneal injection (ip) of a mixture consisting of an equal volume of BSA/AHG, BSA/AHG, BP-BSA/AHG, AMX-BSA/AHG, OXA-BSA/AHG or MEZ-BSA/AHG (50 mg/kg) on days 1, 3 and 5, and challenged by intravenous injection (iv) OVA, BSA, BP-OVA, AMX-OVA, OXA-OVA or MEZ-OVA (50 mg/kg) on day 20, respectively. After the challenge injections were given, the rats were observed for 30 min, and signs of allergies and number of deaths were recorded. The animal experimental design is shown in Supplementary Fig. S1 online.

Blood was immediately withdrawn from the abdominal aorta of deceased rats, while blood was collected from non deceased rats after intravenous injection for 30 min under 2–5% isoflurane anesthesia. All bloods were collected into the general vacuum tube, stood at room temperature for 30 min, and then centrifuged (1200 ×g, 4 ℃) for 10 min. The upper layer (serum) was transferred to cryovials in aliquots, frozen rapidly using liquid nitrogen, and stored at -80 ℃ until analysis.After blood collection, the rats were dissected to collect lung tissue. Each lung tissue specimen was immediately snap-frozen after sampling and stored at -80 ˚C. The frozen samples were subsequently sectioned serially at 6-μm thickness and fixed in acetone for the immunohistochemical analysis.

Allergy model validations.*Assessment of systemic anaphylactic symptoms.* The extent of anaphylactic responses was evaluated on the basis of the occurrence of typical clinical symptoms of anaphylaxis, which were graded as follows[22,31]: no symptom, -; nose rubbing and/or fur erection, ±; weakness, dyspnea, coughing, sneezing, vomiting and/or wheezing, +; convulsion, cyanoses and/or collapse, ++; death within 30 min, +++.

IgE. IgE was measured with ELISA following the manufacturer's instructions of the ELISA kit. Results were expressed as the mean ± standard deviation (SD) and analyzed by one-way analysis of variance (ANOVA) with

Scheffe post-hoc test using IBM SPSS (IBM SPSS Statistics, Armonk, NY, USA, Rev. 21.0). A value of $p < 0.05$ was considered significantly different.

Immunohistochemical detection of tryptase protein in the lung. Sections were treated with 3% hydrogen peroxide for 10 min to block neutralize endogenous peroxidases, followed by 10% goat serum block for 30 min. The sections were then incubated with rabbit anti-mast cell tryptase (dilution1:100) for 12 h at 4 °C. After 3 × 5 min PBS rinses, the horseradish peroxidase polymer solution was added and incubated at 37 °C for 30 min. The antibody binding sites were visualized by incubation with a diaminobenzidine-H_2O_2 solution. Finally, sections were faintly counterstained with hematoxylin. The sections incubated with PBS instead of the primary antibody were used as negative controls. Brown particles in cytoplasm were recognized as positive staining for tryptase.

Metabolomics analysis.*Sample preparation.* Serum samples were thawed before extraction. Then, a total of 500 µL of ice-cooled MeCN and 20µL of 2-chloro-L-phenylalanine (0.1 mg/mL), as the internal standard (IS), were added into 100 µL of serum to remove proteins. After vortex mixing for 1 min and centrifugation (14000×g, 10 min, at 4 °C), 200 µL of the resultant supernatant was withdrawn and freeze-dried in a freeze concentration centrifugal dryer (Eppendorf, Hamburg, Germany). All residues extracted from serum samples were dissolved with 100 µL MeOH, and injected into the UHPLC-MS/MS system. The QC samples were prepared by mixing aliquots of all the supernatants to form a pooled sample for monitoring the stability of analytical method and system.

UHPLC-MS/MS Analysis. The separation and analysis were conducted in an Agilent 1290 Infinity II Series UHPLC (Agilent Technologies, Santa Clara, CA, USA) equipped with an automated multisampler module and a High Speed Binary Pump, coupled to a Mass Spectrometer (Agilent 6550 Q-TOF, Agilent Technologies, Santa Clara, CA, USA) using an Agilent Jet Stream Dual electrospray (AJS-Dual ESI) interface, controlled by the MassHunter Workstation Data Acquisition software (Agilent Technologies, Rev. B.08.00).

The ACQUITY UPLC BEH C18 Column (100 × 2.1 mm, 1.7 µm, Waters, Milford, MA, USA) protected by an ACQUITY UPLC BEH C18 VanGuard Pre-column (5 × 2.1 mm, 1.7 µm, Waters, Milford, MA, USA) were applied in the chromatographic analysis, which was performed at 30 °C with gradient elution at a constant flow rate of 0.3 mL/min using mobile phase A (0.1% HCOOH in H_2O) and mobile phase B (0.1% HCOOH in MeCN). The gradient elution program was as follows: 0–2.0 min 2% B, 2.0–3.0 min 2–25% B, 3.0–5.0 min 25–30% B, 5.0–6.0 min 30–60% B, 6.0–8.0 min 60% B, 8.0–15.0 min 60–98% B, 15.0–18.0 min 98% B, 18.0–18.5 min 98 − 2% B, 18.5–20.5 min 2% B. A needle wash cycle was performed after each injection to remove any possible sample remnants before the next injection. The autosampler was set at 4 ℃ and the injection volume was 5 µL. The mass spectrometer operated in positive mode and in full scan mode from m/z 50 to 1200. The nebulizer gas pressure was set to 35 psi, the drying gas flow was set to 14 L/min at a temperature of 200 °C, and the sheath gas flow was set to 11 L/min at 350 °C. The capillary voltage was set to 4.0 kV and the cone voltage was set to 35 V.

All raw data were collected in continuous mode and corrected in real time using 2-chloro-L-phenylalanine to ensure the accuracy of the collected data (ESI^+ 200.0473).

Data processing and statistical analysis. The raw data acquired from LC-MS was processed to perform peak extraction, alignment, and normalization using the MassHunter Profinder software (Agilent Technologies, Rev. B.10.0). Then a dataset was exported for the statistical analysis analysis. The established dataset was imported into SIMCA software (Umetrics, Umea, Sweden, Rev.14.1) for multivariate statistical analysis. Multivariate analysis including PCA and OPLS-DA. Simultaneously, 200 times response permutation testing was performed to evaluate the quality of OPLS-DA model. Furthermore, one-way ANOVA and the Scheffe multiple comparison test (a post-hoc analysis) was used to evaluate the differences of metabolites using IBM SPSS (IBM SPSS Statistics, Armonk, NY, USA, Rev. 21.0). Criteria for screening differential metabolites were variable importance in projection (VIP) > 1 for the first principal component in the OPLS-DA, and one-way ANOVA with Scheffe's post-hoc test p-value < 0.05. Some available biochemical databases, such as METLIN (http://metlin.scripps.edu/), KEGG (http://www.genome.jp/kegg/)[64–66], LIPID MAPS (http://www.lipidmaps.org/), Chemspider (http://www.chemspider.com) and HMDB (http://www.hmdb.ca/), were used to analyze and identify the potential biomarkers. The pathway enrichment was performed by metaboanalyst (http://www.metaboanalyst.ca). In addition, we randomly split all samples into 70% training set and 30% testing set to assess the overall performance of the model. Predictive power was assessed by confusion matrices and ROC curves associated with AUC values.

Data availability

All data generated or analysed during this study are included in this published article (and its Supplementary Information files).

Received: 17 May 2024; Accepted: 27 September 2024
Published online: 09 October 2024

References

1. Barker, C. I., Germovsek, E. & Sharland, M. What do I need to know about penicillin antibiotics? *Arch. Dis. Child. Educ. Pract. Ed.* **102**, 44–50 (2017).
2. Castells, M., Khan, D. A. & Phillips, E. J. Penicillin allergy. *N Engl. J. Med.* **381**, 2338–2351 (2019).
3. Ramsey, A. Penicillin allergy and Perioperative Anaphylaxis. *Front. Allergy*. **3**, 903161 (2022).
4. Park, M. A. & Li, J. T. Diagnosis and management of penicillin allergy. *Mayo Clin Proc.* 80, 405–410 (2005).
5. Dhopeshwarkar, N. et al. Drug-Induced Anaphylaxis Documented in Electronic Health Records. *J. Allergy Clin. Immunol. Pract.* **7**, 103–111 (2019).
6. Jerschow, E., Lin, R. Y., Scaperotti, M. M. & McGinn, A. P. Fatal anaphylaxis in the United States, 1999–2010: temporal patterns and demographic associations. *J Allergy Clin Immunol.* 134, 1318–1328 e1317 (2014).

7. Li, Z. D., Liu, W. G., Zhao, Z. Q., Shen, Y. W. & Chen, Y. J. [Analysis of 59 anaphylactic death cases]. *Fa Yi Xue Za Zhi*. **31**, 206–210 (2015).
8. Yilmaz, R., Yuksekbas, O., Erkol, Z., Bulut, E. R. & Arslan, M. N. Postmortem findings after anaphylactic reactions to drugs in Turkey. *Am. J. Forensic Med. Pathol.* **30**, 346–349 (2009).
9. Chang, C., Mahmood, M. M., Teuber, S. S. & Gershwin, M. E. Overview of penicillin allergy. *Clin. Rev. Allergy Immunol.* **43**, 84–97 (2012).
10. Bruhns, P. & Chollet-Martin, S. Mechanisms of human drug-induced anaphylaxis. *J. Allergy Clin. Immunol.* **147**, 1133–1142 (2021).
11. Heldring, N., Kahn, L. & Zilg, B. Fatal anaphylactic shock: a review of postmortem biomarkers and diagnostics. *Forensic Sci. Int.* **323**, 110814 (2021).
12. Da Broi, U. & Moreschi, C. Post-mortem diagnosis of anaphylaxis: a difficult task in forensic medicine. *Forensic Sci. Int*. **204**, 1–5 (2011).
13. Del Duca, F. et al. Death due to anaphylactic reaction: the role of the forensic pathologist in an accurate Postmortem diagnosis. *Med. (Kaunas)* **59,** 2184 (2023).
14. Kobek, M. et al. Possibilities of post-mortem diagnostics, including immunodiagnostics, in cases of sudden death due to anaphylactic and anaphylactoid reactions. *Arch. Med. Sadowej Kryminol*. **64**, 102–110 (2014).
15. Nicholson, J. K., Lindon, J. C. & Holmes, E. J. x. 'Metabonomics': understanding the metabolic responses of living systems to pathophysiological stimuli via multivariate statistical analysis of biological NMR spectroscopic data. *Xenobiotica*. **29**, 1181–1189 (1999).
16. Patti, G. J., Yanes, O., Siuzdak, G. & Innovation Metabolomics: the apogee of the omics trilogy. *Nat. Rev. Mol. Cell. Biol.* **13**, 263–269 (2012).
17. Aleidi, S. M. et al. Obesity connected metabolic changes in type 2 Diabetic patients treated with metformin. *Front. Pharmacol.* **11**, 616157 (2020).
18. Khamis, M. M., Adamko, D. J. & El-Aneed, A. Mass spectrometric based approaches in urine metabolomics and biomarker discovery. *Mass Spectrom. Rev.* **36**, 115–134 (2017).
19. Qiu, F. & Zhang, Y. Q. Metabolic effects of mulberry branch bark powder on diabetic mice based on GC-MS metabolomics approach. *Nutr. Metab. (Lond)*. **16**, 10 (2019).
20. Wang, X., Chen, S. & Jia, W. J. C. P. R. Metabolomics in cancer biomarker research. *Curr. Pharmacol. Rep.* **2**, 293–298 (2016).
21. Wei, Z. et al. Application of Q-TOF–MS based metabonomics techniques to analyze the plasma metabolic profile changes on rats following death due to acute intoxication of phorate. *Int. J. Legal Med.* **135**, 1437–1447 (2021).
22. Hu, X. et al. GC–MS-based metabolic profiling reveals metabolic changes in anaphylaxis animal models. *Anal. Bioanal Chem*. **404**, 887–893 (2012).
23. Gu, Y. Y., Shi, L., Zhang, D. D., Huang, X. & Chen, D. Z. Metabonomics delineates allergic reactions induced by Shuang-Huang-Lian injection in rats using ultra performance liquid chromatography-mass spectrometry. *Chin. J. Nat. Med.* **16**, 628–640 (2018).
24. Gao, X. et al. Deciphering biochemical basis of Qingkailing injection-induced anaphylaxis in a rat model by time-dependent metabolomic profiling based on metabolite polarity-oriented analysis. *J. Ethnopharmacol.* **225**, 287–296 (2018).
25. Zhang, K. et al. The Use of Gas Chromatography coupled with high-resolution Mass Spectrometry-based untargeted metabolomics to Discover metabolic changes and help in the determination of Complex causes of death: a preliminary study. *ACS Omega*. **6**, 2100–2109 (2021).
26. Mabilat, C. et al. Improving antimicrobial stewardship with penicillin allergy testing: a review of current practices and unmet needs. *JAC Antimicrob. Resist*. **4**, dlac116 (2022).
27. Pouessel, G. et al. Anaphylaxis mortality in the perioperative setting: Epidemiology, elicitors, risk factors and knowledge gaps. *Clin. Exp. Allergy*. **54**, 11–20 (2024).
28. Turner, P. J. et al. Fatal anaphylaxis: Mortality Rate and Risk factors. *J. Allergy Clin. Immunol. Pract.* **5**, 1169–1178 (2017).
29. Schwartz, L. B., Metcalfe, D. D., Miller, J. S., Earl, H. & Sullivan, T. J. N. E. J. o. M. Tryptase levels as an indicator of mast-cell activation in systemic anaphylaxis and mastocytosis. *N Engl. J. Med.* **316**, 1622–1626 (1987).
30. Khoo, K. L. et al. Plasma and urine metabolite profiling reveals the protective effect of Clinacanthus nutans in an ovalbumin-induced anaphylaxis model: 1H-NMR metabolomics approach. *J. Pharm. Biomed. Anal.* **158**, 438–450 (2018).
31. Park, J. S. et al. Anti-IL-4 monoclonal antibody prevents antibiotics-induced active fatal anaphylaxis. *J. Immunol.* **158**, 5002–5006 (1997).
32. Simopoulos, A. P. The importance of the omega-6/omega-3 fatty acid ratio in cardiovascular disease and other chronic diseases. *Exp. Biol. Med. (Maywood)*. **233**, 674–688 (2008).
33. Whelan, J. & Fritsche, K. Linoleic acid. *Adv. Nutr.* **4**, 311–312 (2013).
34. Marone, G. et al. Prostaglandin D(2) receptor antagonists in allergic disorders: safety, efficacy, and future perspectives. *Expert Opin. Investig. Drugs*. **28**, 73–84 (2019).
35. Pettipher, R. The roles of the prostaglandin D(2) receptors DP(1) and CRTH2 in promoting allergic responses. *Br. J. Pharmacol.* **153** (Suppl 1), S191–199 (2008).
36. Schuligoi, R. et al. CRTH2 and D-type prostanoid receptor antagonists as novel therapeutic agents for inflammatory diseases. *Pharmacology*. **85**, 372–382 (2010).
37. Hirai, H. et al. Prostaglandin D2 selectively induces chemotaxis in T helper type 2 cells, eosinophils, and basophils via seven-transmembrane receptor CRTH2. *J. Exp. Med.* **193**, 255–261 (2001).
38. Kabashima, K. & Narumiya, S. The DP receptor, allergic inflammation and asthma. *Prostaglandins Leukot. Essent. Fat. Acids*. **69**, 187–194 (2003).
39. Takeshita, K. et al. CRTH2 is a prominent effector in contact hypersensitivity-induced neutrophil inflammation. *Int. Immunol.* **16**, 947–959 (2004).
40. Yoshimura-Uchiyama, C. et al. Differential modulation of human basophil functions through prostaglandin D2 receptors DP and chemoattractant receptor-homologous molecule expressed on Th2 cells/DP2. *Clin. Exp. Allergy*. **34**, 1283–1290 (2004).
41. Kobayashi, K. et al. Prostaglandin D2-DP signaling promotes endothelial barrier function via the cAMP/PKA/Tiam1/Rac1 pathway. *Arterioscler. Thromb. Vasc Biol.* **33**, 565–571 (2013).
42. Nakamura, T. et al. Mast cell-derived prostaglandin D(2) attenuates anaphylactic reactions in mice. *J. Allergy Clin. Immunol.* **140**, 630–632e639 (2017).
43. Miyake, Y. et al. Fish and fat intake and prevalence of allergic rhinitis in Japanese females: the Osaka Maternal and Child Health Study. *J. Am. Coll. Nutr.* **26**, 279–287 (2007).
44. Perez-Chacon, G., Astudillo, A. M., Ruiperez, V., Balboa, M. A. & Balsinde, J. Signaling role for lysophosphatidylcholine acyltransferase 3 in receptor-regulated arachidonic acid reacylation reactions in human monocytes. *J. Immunol.* **184**, 1071–1078 (2010).
45. Knuplez, E. & Marsche, G. An updated review of Pro- and Anti-inflammatory properties of plasma lysophosphatidylcholines in the Vascular System. *Int. J. Mol. Sci.* **21,** 4501 (2020).
46. Wang, B. H. et al. Qufeng Xuanbi Formula inhibited benzo[a]pyrene-induced aggravated asthma airway mucus secretion by AhR/ROS/ERK pathway. *J. Ethnopharmacol.* **319**, 117203 (2024).
47. Jiang, S. et al. The immediate adverse drug reactions induced by ShenMai Injection are mediated by thymus-derived T cells and associated with RhoA/ROCK signaling pathway. *Front. Immunol.* **14**, 1135701 (2023).

48. Riento, K. & Ridley, A. J. Rocks: multifunctional kinases in cell behaviour. *Nat. Rev. Mol. Cell. Biol.* **4**, 446–456 (2003).
49. Wang, D. et al. Penilloic acid is the chief culprit involved in non-IgE mediated, immediate penicillin-induced hypersensitivity reactions in mice. *Front. Pharmacol.* **13,** 874486 (2022).
50. Yoder, M. et al. Bioactive lysophosphatidylcholine 16:0 and 18:0 are elevated in lungs of asthmatic subjects. *Allergy Asthma Immunol. Res.* **6**, 61–65 (2014).
51. Baeyens, A., Fang, V., Chen, C. & Schwab, S. R. Exit strategies: S1P Signaling and T Cell Migration. *Trends Immunol.* **36**, 778–787 (2015).
52. Lee, L. Y. & Gu, Q. Role of TRPV1 in inflammation-induced airway hypersensitivity. *Curr. Opin. Pharmacol.* **9**, 243–249 (2009).
53. McGarvey, L. P. et al. Increased expression of bronchial epithelial transient receptor potential vanilloid 1 channels in patients with severe asthma. *J. Allergy Clin. Immunol.* **133**, 704–712e704 (2014).
54. Olivera, A. & Rivera, J. An emerging role for the lipid mediator sphingosine-1-phosphate in mast cell effector function and allergic disease. *Adv. Exp. Med. Biol.* **716**, 123–142 (2011).
55. Barber, D., Villasenor, A. & Escribese, M. M. Metabolomics strategies to discover new biomarkers associated to severe allergic phenotypes. *Asia Pac. Allergy*. **9**, e37 (2019).
56. Laroche, D., Vergnaud, M. C., Sillard, B., Soufarapis, H. & Bricard, H. Biochemical markers of anaphylactoid reactions to drugs. Comparison of plasma histamine and tryptase. *Anesthesiology*. **75**, 945–949 (1991).
57. Onodera, K., Shinoda, H., Imaizumi, M., Hiraki-Sakurai, E. & Yamatodani, A. Effects of intracerebroventricular administration of N-acetylhistamine on body temperature in mice. *Methods Find. Exp. Clin. Pharmacol.* **16**, 575–581 (1994).
58. Xu, Y., Guo, N., Dou, D., Ran, X. & Liu, C. Metabolomics analysis of anaphylactoid reaction reveals its mechanism in a rat model. *Asian Pac. J. Allergy Immunol.* **35**, 224–232 (2017).
59. Hebecker, M. & Jozsi, M. Factor H-related protein 4 activates complement by serving as a platform for the assembly of alternative pathway C3 convertase via its interaction with C3b protein. *J. Biol. Chem.* **287**, 19528–19536 (2012).
60. Zhen, J. et al. The multiomics analyses of gut microbiota, urine metabolome and plasma Proteome revealed significant changes in Allergy featured with Indole Derivatives of Tryptophan. *J. Asthma Allergy*. **15**, 117–131 (2022).
61. Levine, B. B. & Ovary, Z. Studies on the mechanism of the formation of the penicillin antigen. III. The N-(D-alpha-benzylpenicilloyl) group as an antigenic determinant responsible for hypersensitivity to penicillin G. *J. Exp. Med.* **114**, 875–904 (1961).
62. Deak, P. E. et al. Covalent heterobivalent inhibitor design for inhibition of IgE-Dependent penicillin allergy in a murine model. *J. Immunol.* **203**, 21–30 (2019).
63. Paget, G. E. & Barnase, J. M. In *Evaluation of Drug Activities: Pharmaocometrics*. Vol. 1 (eds Laurence, D. R. & Bocharach, A. L.) 3–22 (Academic, 1964).
64. Kanehisa, M. & Goto, S. K. E. G. G. Kyoto Encyclopedia of genes and genomes. *Nucleic Acids Res.* **28**, 27–30 (2000).
65. Kanehisa, M. Toward understanding the origin and evolution of cellular organisms. *Protein Sci.* **28**, 1947–1951 (2019).
66. Kanehisa, M., Furumichi, M., Sato, Y., Kawashima, M. & Ishiguro-Watanabe M. KEGG for taxonomy-based analysis of pathways and genomes. *Nucleic Acids Res.* **51**, D587–D592 (2023).

Acknowledgements

This work was supported by grants from the National Natural Science Foundation of China (grant no. 82130056 and 82072116).

Author contributions

Q.S. and K.Y. conceived and designed the experiments. Q.S., S.W. and G.W. performed the experiments. T.W. contributed reagents and materials. Q.S. and S.W. analyzed and interpreted of data, writing the manuscript. K.D.,C.G. and X.G. contributed to the draft revision process. All authors reviewed the manuscript.

Declarations

Competing interests

The authors declare no competing interests.

Additional information

Supplementary Information The online version contains supplementary material available at https://doi.org/10.1038/s41598-024-74623-x.

Correspondence and requests for materials should be addressed to K.Y.